

# Quasi-condensation and coherence in the quasi-two-dimensional trapped Bose gas

R.N. Bisset<sup>1</sup>, M.J. Davis<sup>2</sup>, T.P. Simula<sup>3</sup>, and P.B. Blakie<sup>1</sup>

<sup>1</sup>*Jack Dodd Centre for Quantum Technology, Department of Physics, University of Otago, New Zealand*

<sup>2</sup>*ARC Centre of Excellence for Quantum-Atom Optics, School of Physical Sciences, University of Queensland, Brisbane, QLD 4072, Australia*

<sup>3</sup>*Department of Physics, Okayama University, Okayama 700-8530, Japan*

(Dated: June 4, 2022)

We simulate a trapped quasi-two-dimensional Bose gas using a classical field method. To interpret our results we introduce two characteristic temperatures determined from our simulations: the condensation temperature  $T_c$  and the uniform Berezinskii-Kosterlitz-Thouless (BKT) temperature  $T_{BKT}$ . We observe that density fluctuations are suppressed in the system above  $T_c$  as a quasi-condensate forms as the first manifestation of degeneracy. At  $T_c$  a coherent condensate forms, which has a clear bimodal structure in momentum space. At  $T_{BKT}$  algebraic decay of off-diagonal correlations occurs near the trap center when the peak density satisfies the uniform condition for the BKT phase transition. Our results provide a comprehensive picture of the low temperature phase diagram of the trapped quasi-2D Bose gas and a consistent interpretation of recent experiments.

PACS numbers: 03.75.Lm, 67.85.De

The physics of two-dimensional systems is very different from what we observe in the three-dimensional world. According to the Mermin-Wagner-Hohenberg theorem [1, 2] in reduced dimensionality thermal fluctuations destroy the long-range order characteristic of most phase transitions. However, in systems that support topological defects, such as vortices, the existence of a quasi-long-range ordered (quasi-coherent) state was predicted to occur by Berezinskii, Kosterlitz and Thouless (BKT) [3, 4]. This superfluid transition has been experimentally observed in liquid helium thin films [5], superconducting Josephson-junction arrays [6] and in spin-polarized atomic hydrogen [7]. More recently evidence for this BKT transition was reported for a dilute gas of  $^{87}\text{Rb}$  atoms by the ENS group [8, 9, 10]. Strong fluctuations, the interplay of harmonic confinement and interactions, and finite size effects have made predictions for the low temperature phase diagram of this system the subject of much debate [11, 12, 13, 14, 15, 16, 17, 18]. Meanfield methods are inapplicable and reliable predictions have only recently become available from classical field and Quantum Monte Carlo methods [19, 20].

As a result of the limited theoretical understanding, the relationship between bimodality in the density distribution [10], algebraic decay of phase coherence [9], and thermal activation of phase defects [8, 9] has been unclear and the subject of speculation. In particular, a crucial issue is that the critical point identified in [10] is distinct from the BKT cross-over found in [9]. In this letter we address this situation by providing a detailed analysis of the low temperature properties of the system. We show that quasi-condensation (i.e. suppression of density fluctuations), and condensation (i.e. spatial coherence) – equivalent phenomena in the 3D gas – are distinct effects in the 2D trapped gas, and are both different from the uniform condition for the BKT transition [13]. We show clear measurable signatures of each effect, and predict that the critical point identified in [10] coincides with condensation, whereas the cross-over observed in [9] occurs where the uniform BKT condition is satisfied. Fig. 1 shows microstates of the quasi-

2D trapped gas in the degenerate regime and indicates important features of this system: In all cases a quasi-condensate (as defined below) is present, and is the only degenerate component for the highest temperature result Fig. 1(a). As the temperature decreases [Fig. 1(b)] a condensate forms. However, in this temperature regime vortices are prolific and we frequently observe free vortices in the condensate. For the lower temperature results (i.e.  $T \lesssim T_{BKT}$ ) [see Figs. 1(c) and (d)] we see that in the central (condensate) region density fluctuations are significantly reduced and vortices and anti-vortices are mostly found paired (i.e. in close proximity).

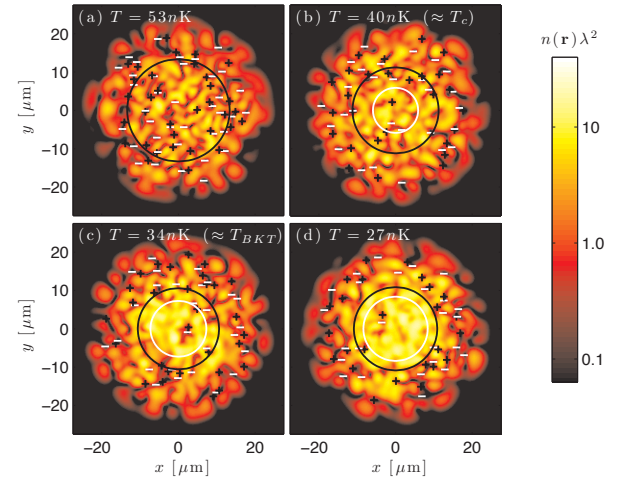


Figure 1: (color online) Instantaneous planar density of a quasi-2D classical field at a range of temperatures. Inner white (outer black) circle marks the  $1/e$ -boundary of the condensate (quasi-condensate) density. Vortices (+) and anti-vortices (-) are shown. Calculation for  $^{87}\text{Rb}$  with  $\omega = 2\pi \times 9.4\text{Hz}$ ,  $\omega_z = 2\pi \times 1.88\text{kHz}$  and  $\bar{g} = 0.107$ .

**Formalism:** Here we consider a harmonically trapped Bose gas described by the Hamiltonian

$$\hat{H} = \int d^3x \hat{\Psi}^\dagger \left\{ H_{sp} + \frac{2\pi a \hbar^2}{m} \hat{\Psi}^\dagger \hat{\Psi} \right\} \hat{\Psi}, \quad (1)$$

where  $H_{sp} = p^2/2m + \frac{1}{2}m\sum_{j=\{x,y,z\}}\omega_j^2x_j^2$ , and  $a$  is the s-wave scattering length. Under tight confinement along the  $z$ -axis, i.e.  $\omega_z \gg \omega_x, \omega_y$  this system becomes quasi-2D, with degrees of freedom along the  $z$ -direction freezing out at sufficiently cold temperatures. It is conventional to define the dimensionless 2D coupling constant as  $\tilde{g} = \sqrt{8\pi}a/a_z$ , with  $a_z = \sqrt{\hbar/m\omega_z}$ . We will assume that  $a_z \gg a$  so that the scattering is approximately three-dimensional [12], a condition well-satisfied in the experiments. In what follows we will take  $\mathbf{r} = (x, y)$  to be the 2D position vector, all densities to be areal (i.e. integrated along  $z$ ), and the trap to be radially symmetric with  $\omega \equiv \omega_x = \omega_y$  the radial trap frequency.

Our simulation method is based upon a classical field (denoted by  $\Phi$ ) representation of the low energy modes of the system. The remaining high energy modes, that we refer to as the *above region*, are described by a quantum field (denoted by  $\hat{\Psi}$ ), as detailed in Ref. [21]. Averages of the full field,  $\hat{\Psi} = \Phi + \hat{\psi}$ , are obtained by time averaging the dynamics of the classical field and ensemble averaging the properties of  $\hat{\psi}$  using a Hartree-Fock meanfield analysis [19, 22, 23]. Because the classical field approach captures the non-perturbative dynamics of the low energy modes it is valid in the critical regime which extends over a large temperature region in the 2D system. Indeed, such a classical analysis was shown to agree with Quantum Monte Carlo results for the uniform case [14]. Features of our approach include its computational efficiency and suitability for studying non-equilibrium dynamics, such as the vortex dynamics shown in Fig. 1.

Recently Holzmann *et al.* [20] have extended a Quantum Monte Carlo method to study this system. In that work they proposed a model for the superfluid component of the system based on a local density application of the uniform results [14]. In detail, they suggest a superfluid density of the form

$$n_{sf}(r) = \begin{cases} \frac{1}{2}(m\omega r_{cr})^2(1 - r^2/r_{cr}^2)/\hbar^2\tilde{g} + \frac{4}{\lambda^2}, & r \leq r_{cr} \\ 0, & r > r_{cr} \end{cases} \quad (2)$$

where  $r_{cr}$  is the radius at which the trapped system density equals the (temperature dependent) critical value

$$n_{cr} = \lambda^{-2} \log(C/\tilde{g}), \quad (3)$$

with  $C = 380 \pm 3$  and  $\lambda = h/\sqrt{2\pi m k_B T}$  ( $n_{cr}\lambda^2$  is the critical phase-space density for the uniform 2D Bose gas to undergo the BKT transition [13]). In [20] Eq. (2) was shown to provide a reasonable description of the moment of inertia obtained directly from Monte Carlo calculations, however this model has curious behavior at the transition whereby the superfluid density discontinuously emerges as a sharp spike when the central (peak) density of the system exceeds  $n_{cr}$ . We denote the temperature where this occurs as  $T_{BKT}$ . We now define the low temperature components of the system, that are of central concern in this paper.

**Quasi-condensate:** is defined as the component of density with suppressed density fluctuations, i.e.  $n_{qc}(\mathbf{r}) = \sqrt{2n(\mathbf{r})^2 - \langle \hat{n}(\mathbf{r})^2 \rangle}$  [14], where  $\hat{n}(\mathbf{r}) = \hat{\Psi}^\dagger(\mathbf{r})\hat{\Psi}(\mathbf{r})$  is the density operator for the system and  $n(\mathbf{r}) = \langle \hat{n}(\mathbf{r}) \rangle$ . There are many

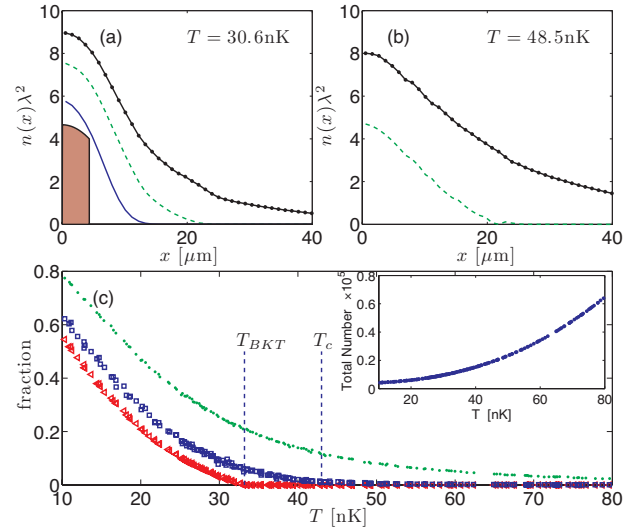


Figure 2: (color online) Component densities at (a)  $T = 30.6 \text{ nK}$  and (b)  $T = 48.5 \text{ nK}$ :  $n(x)$  (dotted-line),  $n_{qc}(x)$  (dashed),  $n_c(x)$  (solid) and  $n_{sf}(x)$  (shaded region). (c) Fraction of atoms in quasi-condensate (dots), condensate (squares) and superfluid (triangles). Inset shows the total atom number. Other parameters as in Fig. 1

imprecise *definitions* of quasi-condensate in the literature involving the notions of suppressed density fluctuations and absence of long range order. The definition we use here was shown to furnish a universal quantity in the uniform gas [14].

**Condensate:** is defined using the Penrose-Onsager procedure, i.e. by diagonalising the one-body density matrix  $G = \langle \hat{\Psi}^\dagger(\mathbf{r})\hat{\Psi}(\mathbf{r}') \rangle$  and assigning the largest eigenvalue (eigenvector) as the condensate population (mode), e.g. see [21, 24]. We denote the temperature at which a condensate emerges in the system as  $T_c$  and the condensate density as  $n_c(\mathbf{r})$ .

**Results:** Fig. 2 shows the results of our analysis for a system with  $\tilde{g} = 0.107$ . Our simulation is for a fixed classical region which results in a varying total atom number (shown in inset). Figs. 2(a) and (b) show density profiles of the system at two temperatures. In Fig. 2(a) quasi-condensate and condensate components are present, where as Fig. 2(b) is at a higher temperature where only quasi-condensate is present. Fig. 2(c) summarizes the degenerate components of the system over a large temperature range. At the highest temperatures we observe a small quasi-condensate fraction, which increases with decreasing temperature. At temperatures below  $T_c \approx 43 \text{ nK}$  the condensate fraction becomes appreciable (for the same number of atoms the ideal gas transition is about  $44 \text{ nK}$ ). In this regime we commonly see *free* vortices in the condensate [e.g. see Fig. 1(b)] which will likely have a profound effect on its coherence properties. Finally, at  $T_{BKT} \approx 34 \text{ nK}$  the peak density (at the trap center) satisfies Eq. (3) and the model, Eq. (2), predicts a non-zero superfluid fraction. Here we observe the occurrence of vortices in the condensate to be much less frequent than at higher temperatures, and those found are usually paired [e.g. see Fig. 1(c) and (d)]. As the temperature decreases further, the quasi-condensate, condensate and

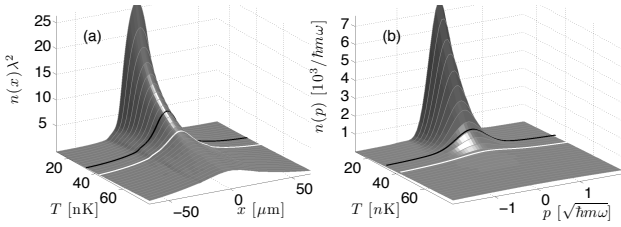


Figure 3: Density distributions versus temperature. (a) Position phase-space density and (b) momentum space density distributions. The black (white) curves mark the densities at  $T_{BKT}$  ( $T_c$ ) [also see Fig. 2]. Parameters as in Fig. 1

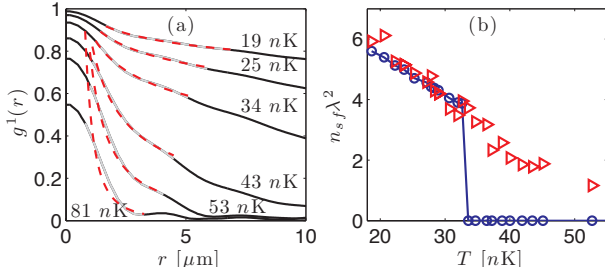


Figure 4: (color online) (a)  $g^1(r)$  for various temperatures (solid lines). Fitting region (light colored segments of curves) and algebraic fits (dashed) are also shown. (b) Peak superfluid density determined from fits to algebraic decay (triangles) and from model density, Eq. (2) (circles). Parameters as in Fig. 1

superfluid fractions become more similar, though are always clearly distinguishable.

An important result of this paper is that the condensation temperature,  $T_c$ , is well above the uniform system superfluidity temperature,  $T_{BKT}$ , i.e. the emergence of spatial coherence in the trapped system occurs before the peak phase space density satisfies Eq. (3). We have carried out simulations for  $\tilde{g}$  values in the range 0.02 to 0.107 and observe similar results.

In Fig. 3 we show the position and momentum density distributions corresponding to the above results. In Fig. 3(a) the (position space) phase-space density is seen to smoothly peak as the temperature decreases [28]. We have confirmed that at low temperatures the central density is well-described by a Thomas-Fermi-like profile of the form  $n(r) \sim n(0) - m^2 \omega^2 r^2 / 2\hbar^2 \tilde{g}$  (also see [20]). Additionally, we observe that whenever appreciable quasi-condensate is present the density profile clearly bulges (e.g. see Fig. 2(b)). Fig. 3(b) shows that for temperatures above  $T_c$  a strong bimodality is apparent in the momentum space density of the system associated with the extended spatial coherence arising from the condensate. We emphasize that this bimodality is clearly apparent at temperatures well-above  $T_{BKT}$ .

**Decay of coherence:** An important prediction of the Kosterlitz-Thouless theory for the uniform system is that in the superfluid regime off-diagonal correlations (phase coherence) decay algebraically, i.e.  $G(r) \sim r^{-\alpha}$ , where  $r$  is the spatial separation and the exponent relates to the superfluid density as  $\alpha = 1/n_{sf}\lambda^2$ . At  $T_{BKT}$  the superfluid transition oc-

curs with  $n_{sf}\lambda^2 = 4$  (i.e.  $\alpha = 0.25$ ) and at temperatures above  $T_{BKT}$  the system is normal with exponentially decaying correlations.

Here we investigate the nature of off-diagonal correlations in the trapped system [25]. Because of spatial inhomogeneity the first order correlation function depends on centre-of-mass and relative coordinates, and we therefore choose to examine these correlations at the trap center. Thus the normalized correlation function we evaluate is

$$g^1(\mathbf{r}) = \frac{\langle \Phi^*(\frac{\mathbf{r}}{2}) \Phi(-\frac{\mathbf{r}}{2}) \rangle}{\sqrt{n(\frac{\mathbf{r}}{2}) n(-\frac{\mathbf{r}}{2})}}, \quad (4)$$

comparing points symmetrically placed about the origin [29]. Typical results for this correlation function for a range of temperatures are shown in Fig. 4(a). We least-squares fit a model decay curve of the form  $cr^{-\alpha}$  to  $g^1(r)$  over the spatial range  $1.2\lambda < r < 5\lambda$  to determine the exponent  $\alpha$  (with  $c$  a constant fit parameter). The lower spatial limit excludes the short range contribution of normal-component atoms, while the upper limit restricts the effects of spatial inhomogeneity (typical size of cloud is of order  $30\lambda$ ). The model fits [shown in Fig. 4(a)] are poor in the three highest temperature cases, suggesting that the algebraic fit is inappropriate. Using the fitted values of  $\alpha$  we infer the superfluid density at trap center according to  $n_{sf}(0) = (\alpha\lambda^2)^{-1}$ . These results (shown in Fig. 4(b)) compare well with the peak of the model superfluid density, Eq. (2), for temperatures below  $T_{BKT}$ . At higher temperatures (where  $n(0) < n_{cr}$ ) the two results disagree, however in this temperature range the algebraic fit is poor and an exponential fit appears to be more appropriate.

**Relation to experiments:** Our results allow us to interpret the experiments of the ENS group. In the most recent experiment Krüger *et al.* [10] determined the “exact critical point” by observing bimodality in the density distribution after expansion. Two key results of this critical point were that (i) a large shift in the critical temperature from the ideal condensation temperature was measured; (ii) the occurrence of bimodality coincided with the appearance of interference fringes when two such systems overlapped. Point (i) has been largely resolved in a subsequent work [26] that revised the method for extracting temperatures from density images of the system. Here we focus on point (ii). The experimental procedure was to release the gas for 22 ms of time-of-flight before absorption imaging was used to measure the system density. This time scale is of order the characteristic time for expansion in the weak trap direction ( $\omega_x \approx 2\pi \times 9.4$  Hz) and so the measured density distribution along  $x$  is in an intermediate regime not well-represented by the *in situ* spatial or momentum densities, but in some sense combining the features of both. A semiclassical analysis of this expansion is presented in [26].

While the quasi-condensate exhibits a certain amount of spatial bulging, the sharp bimodal feature seen in the experiment (Fig. 2 of [10]) is almost certainly due to the onset of condensation (see Fig. 3(b)). This prediction could be verified using longer expansion times to more clearly reveal the con-

densate. Identifying this critical point with the condensation transition also allows us to understand the onset of interference. In the quasi-2D regime,  $k_B T \lesssim \hbar \omega_z$ , the two interfering systems should produce fringes along  $z$  with high (local) contrast, however the location and amplitude of these fringes will vary in the  $xy$ -plane due to fluctuations across each system. These local fringes are averaged over the  $y$ -direction in an absorption image (a column density along  $y$ ) and reduce the contrast in the observed interference pattern. Thus the imaged column density will exhibit appreciable interference fringes when the coherence length is of order the  $y$ -extent of the system. As the  $y$ -direction is the tighter of the weakly trapped directions (with  $\omega_y \approx 2\pi \times 125\text{Hz}$ ), this can occur well before the coherence length is comparable to the system's  $x$ -extent. Such spatial coherence grows rapidly at temperatures below  $T_c$  with the formation of a condensate (e.g. the rapid change in spatial coherence observed between the  $T = 43\text{nK}$  and  $T = 34\text{nK}$  curves in Fig. 4(a)). This leads us to conclude that the observations of bimodality and interference in experiment coincides with  $T_c$ .

In an earlier experiment [9] the BKT transition was located by using a heterodyning scheme to determine when off-diagonal correlations in the central region of the system had an algebraic decay coefficient of  $\alpha \approx 0.25$ . This condition was achieved at temperatures well below where interference fringes were first observed, and thus differs from the critical point of [10]. Our results in Fig. 4 show that  $\alpha = 0.25$  occurs where the peak density satisfies Eq. (3), which we have used to define  $T_{BKT}$ . Interestingly it is speculated in [10] that the onset of bimodality ( $T_c$ ) should coincide with the uniform prediction for superfluidity, Eq. (3), whereas our results show that the latter occurs at the lower temperature of  $T_{BKT}$ .

**Conclusions and outlook:** In this paper we have provided a comprehensive analysis of the low-temperature properties of the trapped 2D Bose gas and have elucidated the role of condensation and quasi-condensation in the system. A major issue that remains to be dealt with is the nature of superfluidity in this system. A model for the superfluid density was proposed by Holzmann *et al.* [20] who showed that it provided a reasonable description of the system's moment of inertia. Our results suggest that in the temperature range  $T_{BKT} < T < T_c$  a condensate exists yet the model (and uniform system) criterion for superfluidity is not fulfilled. It would be of interest to determine whether a system in this regime is superfluid. The answer is far from clear as the condensate is often penetrated by vortices in this temperature range [e.g. see Fig. 1(b)] which may act to destroy its superfluidity. Indeed, recent experimental studies in this regime observe a bimodal density profile with strong phase fluctuations, a feature they term as a *fractured quasi-condensate* [27].

Our calculations for the off-diagonal correlations in the system reveal that extended coherence emerges at  $T_c$ , whereas the field develops algebraically decaying correlations, accurately described by the superfluid model, at lower temperatures  $T \lesssim T_{BKT}$ . Our results also provide a clear interpretation of the differences between the transitions identified in

Refs. [9, 10].

Having mapped out the low temperature components of the system, in future work we will concentrate on dynamics, in particular the role of vortices and density fluctuations. As shown in Fig. 1, the classical field microstates capture the creation of vortices and their ensuing dynamics. We will use our calculations to clarify the nature of pairing between vortices, their typical production rate and lifetime, enabling us to better understand their role in the equilibrium state.

The authors acknowledge valuable discussions with the ENS and NIST groups. PBB and RNB are supported by NZ-FRST contract NERF-UOOX0703. TPS acknowledges support from JSPS. MJD acknowledges support from the Australian Research Council.

- 
- [1] N. D. Mermin and H. Wagner, Phys. Rev. Lett. **17**, 1133 (1966).
  - [2] P. C. Hohenberg, Phys. Rev. **158**, 383 (1967).
  - [3] V. L. Berezinskii, Sov. Phys. JETP **32**, 493 (1971).
  - [4] J. M. Kosterlitz and D. J. Thouless, J. Phys. C: Solid State Physics **6**, 1181 (1973).
  - [5] D. J. Bishop and J. D. Reppy, Phys. Rev. Lett. **40**, 1727 (1978).
  - [6] D. J. Resnick, J. C. Garland, J. T. Boyd, S. Shoemaker, and R. S. Newrock, Phys. Rev. Lett. **47**, 1542 (1981).
  - [7] A. I. Safonov, S. A. Vasilyev, I. S. Yasnikov, I. I. Lukashevich, and S. Jaakkola, Phys. Rev. Lett. **81**, 4545 (1998).
  - [8] S. Stock, Z. Hadzibabic, B. Battelier, M. Cheneau, and J. Dalibard, Phys. Rev. Lett. **95**, 190403 (2005).
  - [9] Z. Hadzibabic, P. Krüger, M. Cheneau, B. Battelier, and J. Dalibard, Nature **441**, 1118 (2006).
  - [10] P. Krüger, Z. Hadzibabic, and J. Dalibard, Phys. Rev. Lett. **99**, 040402 (2007).
  - [11] V. N. Popov, *Functional Integrals in Quantum Field Theory and Statistical Physics* (Reidel, Dordrecht, 1983).
  - [12] D. S. Petrov, M. Holzmann, and G. V. Shlyapnikov, Phys. Rev. Lett. **84**, 2551 (2000).
  - [13] N. Prokof'ev, O. Ruebenacker, and B. Svistunov, Phys. Rev. Lett. **87**, 270402 (2001).
  - [14] N. Prokof'ev and B. Svistunov, Phys. Rev. A **66**, 043608 (2002).
  - [15] J. O. Andersen, U. Al Khawaja, and H. T. C. Stoof, Phys. Rev. Lett. **88**, 070407 (2002).
  - [16] C. Gies, B. P. van Zyl, S. A. Morgan, and D. A. W. Hutchinson, Phys. Rev. A **69**, 023616 (2004).
  - [17] A. Trombettoni, A. Smerzi, and P. Sodano, New J. Phys. **7**, 57 (2005).
  - [18] T. P. Simula, M. D. Lee, and D. A. W. Hutchinson, Philos. Mag. Lett. **85**, 395 (2006).
  - [19] T. P. Simula and P. B. Blakie, Phys. Rev. Lett. **96**, 020404 (2006).
  - [20] M. Holzmann and W. Krauth, <http://arxiv.org/abs/0710.5060>.
  - [21] P. B. Blakie and M. J. Davis, Phys. Rev. A **72**, 063608 (2005).
  - [22] M. J. Davis and P. B. Blakie, Phys. Rev. Lett. **96**, 060404 (2006).
  - [23] T. P. Simula, M. J. Davis, and P. B. Blakie, Phys. Rev. A **77**, 023618 (2008).
  - [24] O. Penrose and L. Onsager, Phys. Rev. **104**, 576 (1956).
  - [25] A. Bezett, E. Toth, and P. B. Blakie, Phys. Rev. A **77**, 023602 (2008).

- [26] Z. Hadzibabic, P. Krüger, M. Cheneau, S. P. Rath, and J. Dalibard, <http://arxiv.org/abs/0712.1265>.
- [27] P. Cladé, C. Ryu, A. Ramanathan, K. Helmerson, and W. D. Phillips, in preparation.
- [28] The low temperature peaking of phase-space density is significantly enhanced over that of the bare density since  $\lambda$  increases as  $T$  decreases.
- [29] The numerator of  $g^1$  neglects the above atom contribution, whereas the denominator contains the total density. As the above region correlation length is  $\lambda$ , this approximation is good for  $r \gtrsim \lambda$  (see [23, 25]).